

# Mechanical Properties of Single-Brin Silkworm Silk

J. PÉREZ-RIGUEIRO,<sup>1</sup> C. VINEY,<sup>2</sup> J. LLORCA,<sup>1</sup> M. ELICES<sup>1</sup>

<sup>1</sup> Departamento de Ciencia de Materiales, Universidad Politécnica de Madrid, ETS de Ingenieros de Caminos, Ciudad Universitaria, 28040 Madrid, Spain

<sup>2</sup> Department of Chemistry, Heriot-Watt University, Edinburgh EH14 4AS, Scotland

Received 12 May 1999; accepted 19 June 1999

**ABSTRACT:** Mechanical tests were performed on single brins of *Bombyx mori* silkworm silk, to obtain values of elastic modulus ( $E$ ), yield strength, tensile breaking strength, and shear modulus ( $G$ ). Specimen cross-sectional areas, needed to convert tensile loads into stresses, were derived from diameter measurements performed by scanning electron microscopy. Results are compared with existing literature values for partially degummed silkworm baves. The tensile modulus ( $16 \pm 1$  GPa) and yield strength ( $230 \pm 10$  MPa) of *B. mori* brin are significantly higher than the literature values reported for bave. The difference is attributed principally to the presence of sericin in bave, contributing to sample cross-section but adding little to the fiber's ability to resist tensile deformation. The two brins in bave are found to contribute equally and independently to the tensile load-bearing ability of the material. Measurements performed with a torsional pendulum can be combined with tensile load-extension data to obtain a value of  $E/\sqrt{G}$  that is not sensitive to sample cross-sectional dimensions or, therefore, to the presence of sericin. The value of  $E$  measured for brin can be used together with this result to obtain  $G = 3.0 \pm 0.8$  GPa and  $E/G = 5.3 \pm 0.3$  for brin. The latter value indicates a mechanical, and therefore microstructural, anisotropy comparable to that of nylon. © 2000 John Wiley & Sons, Inc. *J Appl Polym Sci* 75: 1270–1277, 2000

**Key words:** bave; brin; shear modulus; silkworm silk; tensile modulus

## INTRODUCTION

Silkworms (*Bombyx mori*) produce their cocoon silk from two modified salivary glands. The ducts that lead from these glands are separated along most of their length (approx. 5 cm), merging into a single duct at the spinneret.<sup>1,2</sup> This anatomy leads to the production of a double-thread fiber that is conventionally described as a bave; each of the two constituent monofilaments is called a brin. Both brins originate within the glands as solubilized fibroin, which coagulates during the spinning process. The brins are coated with an

amorphous protein, sericin, as the fibroin leaves the glands. Thermochemical (degumming) treatments<sup>3,4</sup> are, therefore, used in the textile industry to recover bave from cocoons.

Tensile properties of silkworm silk are usually measured from a load-extension test performed on bave. A significant challenge—the need to determine the bave cross-sectional area accurately—is encountered when one attempts to convert these data into a stress–strain plot. The irregular cross-section shape varies with position along the bave, as does the average diameter. Almost all published stress–strain data for silkworm silk rely on relatively crude estimates of the bave area. These estimates are obtained by measuring the mass of one or more segments of bave for which the total length is known, and combining

---

Correspondence to: J. Pérez-Rigueiro.

*Journal of Applied Polymer Science*, Vol. 75, 1270–1277 (2000)  
© 2000 John Wiley & Sons, Inc. CCC 0021-8995/00/101270-08

this information with a measurement of density.<sup>5–8</sup> This approach provides an averaged value of bave cross-sectional area, but is poorly suited to a material that has a highly variable cross-sectional geometry; it is of little use in characterizing the actual cross-section of an individual sample in a tensile test. Indeed, recent studies by scanning electron microscopy (SEM) have demonstrated that diameter can vary by more than a factor of 2 among samples of bave recovered from a single cocoon.<sup>9</sup>

Even if scanning electron microscopy is used to characterize the geometry of individual test samples, some problems remain. Although degumming allows bave to be unravelled from the cocoon, it neither guarantees removal of all the sericin from the surface of the bave, nor achieves complete separation of the constituent brins. The two brins remain intertwined (several times within a centimeter distance) and patchily glued together in bave which is used to produce textile yarns, and which conventionally is characterized in tensile tests. There are two important consequences if one is interested<sup>10</sup> in the engineering properties of silk fibroins. First, it can be difficult to distinguish the perimeter of the individual fibroin core of each brin. Second, the implicit assumptions made in plotting stress–strain curves from tensile tests performed on bave—i.e., that the two brins are parallel, exhibiting the same mechanical properties, undergoing the same deformation, contributing equally and independently to the load-bearing cross-section of the bave—must be questioned. These issues must also be considered if a torsional pendulum is used to quantify the shear modulus of *B. mori* silk, because the shape as well as the area of the bave cross-section can influence the result, as may the imperfect coupling between the constituent brins.

In this article, we describe how individual brins were extracted from *B. mori* silk cocoons and characterized to determine their tensile stress–strain behavior and also their shear modulus. The cross-sectional geometry is determined directly from individual test specimens by SEM. The tensile test results are compared with data obtained previously<sup>9</sup> from *B. mori* bave.

## EXPERIMENTAL

### Obtaining Samples for Mechanical Tests

Silkworm cocoons were boiled in distilled water for 30 min, and 15–25-cm lengths of fiber were

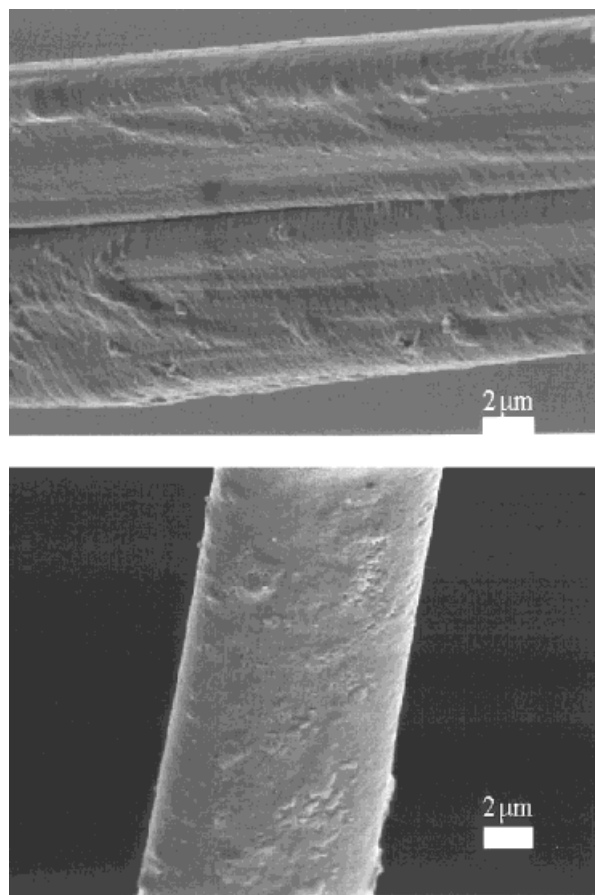


**Figure 1** Micrographs of *B. mori* cocoon silk obtained by scanning electron microscopy: (a) bave, with both brins clearly identifiable; (b) a single brin.

obtained by pulling gently with a pair of tweezers. Care was taken to avoid stretching the fibers plastically during this process. The fibers were allowed to dry in air. Most fibers were baves, but individual brins were sometimes recovered, as observed initially under optical magnification and confirmed by SEM after mechanical testing (Fig. 1). On rare occasions, it was possible to identify free brins at one end of a bave, in which case the brins were separated by gently pulling their free ends simultaneously (see insert in Fig. 5).

### Tensile Testing

Each sample was glued (Loctite 401) across a rectangular hole cut into a cardboard support, to give a gauge length of 40 mm. The support was mounted in an Instron 4411 tensile testing machine, after which the vertical edges of the support were cut so that all the load was transmitted through the fiber. An electronic balance (Precisa

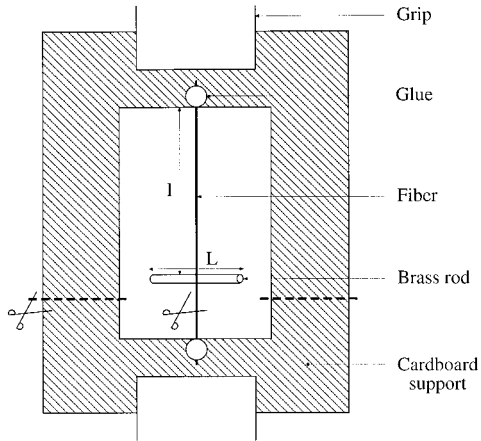


**Figure 2** Schematic representation of the experimental setup used to measure shear modulus.

6100 C; resolution  $\pm 10$  mg) under the lower grip was used instead of a conventional load cell to measure force. Sample elongation was determined as the crosshead displacement (resolution  $\pm 10$   $\mu\text{m}$ ), because the compliance of the mechanical testing machine is negligible compared to that of the sample. The nominal strain rate was fixed at 0.0002/s. Ambient temperature and relative humidity were 20°C and 60%, respectively.

Nominal strains  $\epsilon$  were calculated as the sample elongation divided by the initial length. Nominal stresses were obtained from the load and the initial fiber cross sectional area,  $A_0$ . Consistent with our previous work,<sup>9</sup>  $A_0$  was obtained by assuming that the sample volume remains constant during the test, so that

$$A_0 = A_f l_f / l_0 \quad (1)$$

where  $A_f$  is the final cross-sectional area (calculated as  $\pi D^2/4$  from the mean apparent diameter  $D$  as characterized by SEM after tensile testing), and  $l_0$  and  $l_f$  are the initial and final lengths of the sample.

### Torsional Pendulum

Values of shear modulus were obtained by building samples into a torsional pendulum (Fig. 2). Samples were glued onto the same type of cardboard support as used in tensile tests, to give a 40-mm working length. A small brass rod (length  $L = 12.8$  mm, diameter  $\phi = 2.7$  mm, mass  $m = 0.275$  g) was then glued at its midpoint to the sample, at a point 30 mm from one of the fixed ends of the sample. The moment of inertia,  $I$ , of

the rod was  $(4.22 \pm 0.07) \cdot 10^{-9}$   $\text{kg} \cdot \text{m}^2$ , taking into account that the rotation axis did not coincide with a principal axis but was displaced by  $\phi/2 = 1.35$  mm. The support card was held in the testing machine grips; both vertical edges of the card were then cut, as was the sample below the brass rod, creating a free torsional pendulum with the 30-mm intact length of silk. The period of oscillation was determined from the time required to complete six oscillations. Measurements were repeated, and results from a given sample were only used if the two measurements of oscillation period differed by less than 5%.

### Characterizing Sample Diameters

After mechanical testing, samples were metalized with gold and observed in a JEOL 6300 scanning electron microscope to confirm the sample type (brin or bave), and to determine a mean diameter for each sample. The operating voltage and beam current were 10 kV and 0.6 nA, respectively.

Brin diameter was measured at three different positions along each fiber; at each position characterized, the fiber was observed in two orientations related by a 50° rotation of the fiber about its long axis. (The exact value of this rotation is not important, provided that the two orientations differ significantly.<sup>11</sup> The value of 50° was an instrumentation-imposed upper limit). A mean diameter for the sample was calculated as the average of these six measurements.

In our previous study of *B. mori* silk,<sup>9</sup> where mechanical properties of *bave* were characterized, an average brin diameter was derived from six measurements similarly performed at positions where the brins could be distinguished clearly. However, it was necessary in that case to multiply the approximated brin cross-sectional area by a factor of two to estimate the bave cross-section, with the implicit assumption that the brins contributed equally and independently to the load-bearing capacity of the samples.

## RESULTS AND DISCUSSION

### Tensile Properties of Individual Brins

The stress–strain curves shown in Figure 3 were obtained from tests performed on 10 samples of individual brin. The elastic modulus  $E$ , yield strength  $\sigma_y$  (defined conventionally as the stress

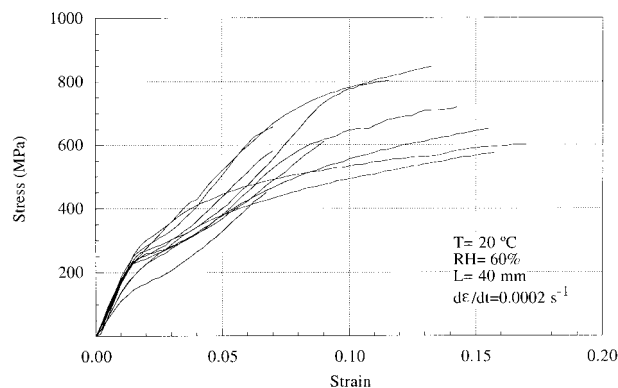


**Figure 3** Stress–strain plots of single brins of *B. mori* silk. Sample diameters measured from micrographs such as Figure 1(b) were used to convert values of force, as recorded during tensile tests, into values of nominal (engineering) stress.

intercept with a line of slope  $E$  drawn through  $\epsilon = 0.002^{12}$ ) and tensile strength  $\sigma_u$  were obtained from these plots; mean values and corresponding standard deviations are shown in Table I.

The elastic modulus determined from single brins is significantly higher than the 5 to 12 GPa range of values reported for *B. mori* silk by other authors.<sup>5–8</sup> In addition, the tensile strength of brin is significantly higher than the literature value of 500 MPa<sup>7,8</sup> usually quoted for *B. mori* silk. When making these comparisons, we are confronted with limited information about the physical condition of the samples that provided the literature values. From the descriptions of protocols used to recover fiber from cocoons, it can be inferred that results pertain to bave, i.e., intertwined brins still at least partially coupled by amorphous sericin. In other words, the published stiffness and strength pertain to a fibroin–sericin composite in which as much as 25% of the cross-section<sup>10</sup> contributes little to its load-bearing ability. The results presented in Figure 3 and Table I for isolated brins are more representative of the properties of fibroin, the effective removal of sericin being confirmed in the SEM. If the top-of-the-range literature values of stiffness and break-

**Table I** Tensile Properties Averaged from Tests Performed on 10 Samples of Individual Brin

$E$ (GPa)	$\sigma_y$ (MPa)	$\sigma_u$ (MPa)
$16 \pm 1$	$230 \pm 10$	$650 \pm 40$

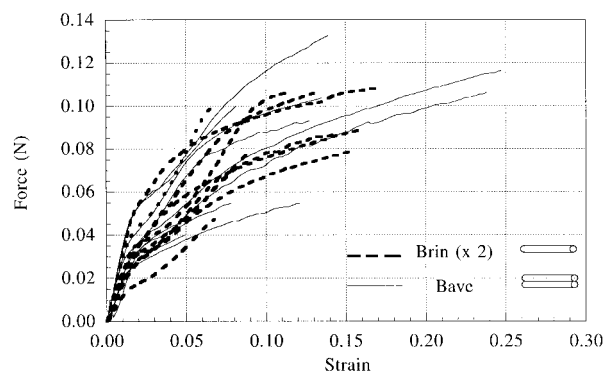


**Figure 4** Comparison of the force–strain plots obtained from baves and brins. Values of force carried by brins have been multiplied by 2, so that the bave and brin data could be superimposed on the same axes.

ing strength are multiplied by a factor of 4/3 ( $=1/0.75$ ) to allow for the presence of sericin in bave, we obtain numbers that fall within the range of our experimental data for brins.

In general, if tensile loads are carried predominantly by the fibroin component of silk, mechanical properties that involve scaling by cross-sectional area will be underrepresented when sericin also contributes to that cross-section. This point is reinforced by Figure 4: the load–strain data for brins that were used to compile Figure 3 have been rescaled vertically by a factor of 2, and are superimposed on our previously published<sup>9</sup> load–strain data for baves. The behavior of brins and baves is seen to be equivalent within the experimental scatter when assessed in terms of load-bearing ability rather than stress-bearing ability. (The scatter itself is principally due to the fact that the cross-section of fibroin is not constant among the samples tested.)

The necessary distinction between load-bearing cross-section and actual cross-section is further reinforced if we consider the geometrical characteristics of the samples used in our previous study of bave and our present study of brin. Table II lists details about the geometry of the brin samples. Shape anisotropy is computed as

**Table II** Brin Cross-Sectional Geometry (Data from 10 Samples)

$D$ ( $\mu\text{m}$ )	Max $D$ ( $\mu\text{m}$ )	Min $D$ ( $\mu\text{m}$ )	Shape Anisotropy
$9.3 \pm 0.3$	11.6	6.7	$1.16 \pm 0.03$

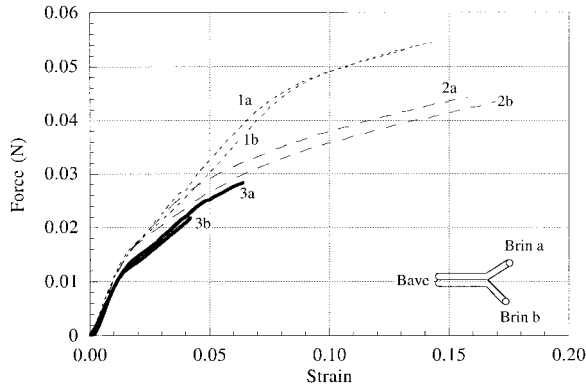


**Figure 5** Force–strain plots obtained from the individual brins in three samples of bave. Within each bave, the two brins follow similar force–strain curves.

the ratio of  $D_0$  (or  $D_{50}$ , whichever number is greater) to  $D_{50}$  (or  $D_0$ , whichever number is smaller); subscripts denote SEM stage rotation about the fiber long axis. Shape anisotropy therefore is an indicator of the departure from a circular cross-section. The average diameter of the individual brin samples ( $9.3 \pm 0.3 \mu\text{m}$ ) is notably smaller than that ( $11.5 \pm 0.2 \mu\text{m}$ ) measured from locally distinguishable brin in samples of bave,<sup>9</sup> where significant quantities of sericin were often retained.

When, in a previous study, our own data for baves were presented as stress–strain curves, we noted<sup>9</sup> that three distinct ranges of both elastic modulus and yield strength could be identified. The highest of these ( $E = 17.4 \pm 0.4 \text{ GPa}$  and  $\sigma_y = 231 \pm 14 \text{ MPa}$ ) corresponds closely to our present results obtained from brins; we believe that the sericin had been effectively removed by the degumming treatment in those cases. This correspondence between brin and well-degummed bave validates the assumption that both brins in a bave exhibit the same intrinsic mechanical properties. Further validation is obtained by measuring independently the force–displacement curves for both brins in a bave, which is possible if the brins are free and identifiable at one end of the bave, allowing them to be separated for individual testing. The results for the three instances in which this was achieved are shown in Figure 5; they demonstrate clearly that individual brins from the same original bave have comparable stiffnesses and yield strengths. At the same time, we note that paired brins can have significantly different breaking strengths, confirming our earlier<sup>9</sup> bave-based conclusion that the fracture properties of *B. mori* silk are poorly reproducible

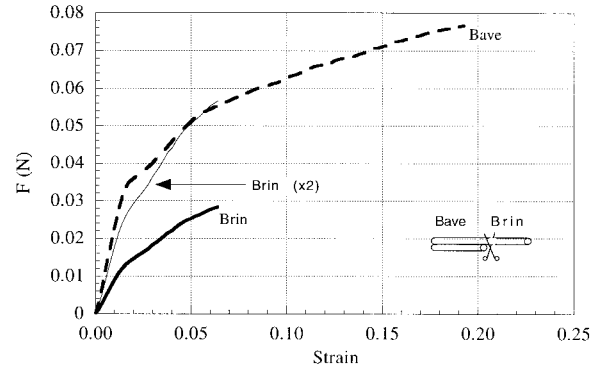


**Figure 6** Comparison of the force–strain characteristics of a bave and one adjacent brin. Doubling the ordinates of the brin data yields a plot that approximately follows the bave data.

and governed by microstructural defects rather than by intrinsic limitations of the silk polymer.

Figures 6 and 7 provide alternative demonstrations that the load is shared equally by both brins in a bave. Because the intrinsic mechanical properties of silk (dragline from spiders<sup>13</sup> as well as from silkworms<sup>9</sup>) vary over a length scale that is greater than the length of our tensile test specimens, the behavior of adjacent (sequential) specimens is expected to be comparable. Figure 6 displays tensile data obtained from bave and an adjacent sample of brin. The load carried by the bave at a given strain is seen to be approximately twice the load supported by the single brin. However, as in Figure 5, the poor reproducibility of the load needed to fracture the silk is apparent. Figure 7 presents two tensile tests conducted on

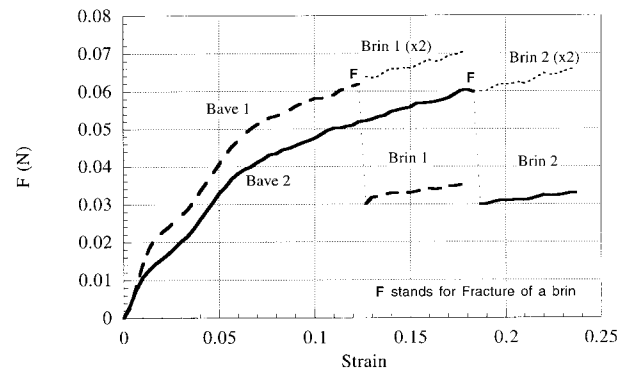


**Figure 7** Tensile test data for baves; in each case one brin fractures during the test while the other remains load bearing. If, after fracture of the first brin, the ordinates of the data for the second brin are doubled, the resulting plot follows the extrapolated trajectory of the bave.

bave: in each case one brin broke while the other remained intact. It is evident that each brin supported one-half of the load carried by the bave.

### Measurement of Shear Modulus

A torsional pendulum has been used to measure the shear modulus of many types of polymer fiber,<sup>12</sup> including silk.<sup>14</sup> The shear modulus can be obtained from the period of oscillation of the pendulum via the following equation:

$$G = \frac{8\pi^3 IL}{\epsilon T^2 A^2} \quad (2)$$

where  $L$  and  $I$ , respectively, are the length and the moment of inertia of the torsional pendulum (Fig. 2),  $A$  is the area of the fiber cross-section, and  $\epsilon$  is a factor that relates to the shape of the cross-section.<sup>14</sup> For a circular cross-section,  $\epsilon = 1$ .

We know (Table II; refs. 15 and 16) that the cross-section of *B. mori* brin is not circular. A better approximation is obtained by fitting an ellipse or an oval. If we assume that the shape anisotropy in Table II always represents the extreme case of  $r/b$ , where  $b$  is the semiminor axis, and  $r$  is the length of a radius vector rotated by  $50^\circ$  relative to the semiminor axes, then it is possible to calculate the length  $a$  of the semimajor axis. The necessary equations<sup>11</sup> in polar coordinates are:

$$r^2 = \frac{a^2 b^2}{a^2 \sin^2 \theta + b^2 \cos^2 \theta} \quad \text{for an ellipse} \quad (3a)$$

$$r = a \cos^2 \theta + b \sin^2 \theta \quad \text{for a simple oval} \quad (3b)$$

In both of these equations,  $\theta$  is measured from the semimajor axis. We substitute  $b = 1$ ,  $r = 1.16$  (from Table II), and  $\theta = 40^\circ (= 90 - 50^\circ)$  into these equations to find  $a$  (and therefore  $a/b$ ) equal to 1.33 for the ellipse and 1.27 for the oval. Given these maximum values of ellipticity and ovality (they are less than 1.5), the brin cross-section can be closely approximated by a circle having as its diameter the average of the experimentally measured values.<sup>11</sup> If  $R$  is half of this diameter, eq. (2) can be replaced by:

$$G = \frac{8\pi IL}{T^2 R^4} \quad (4)$$

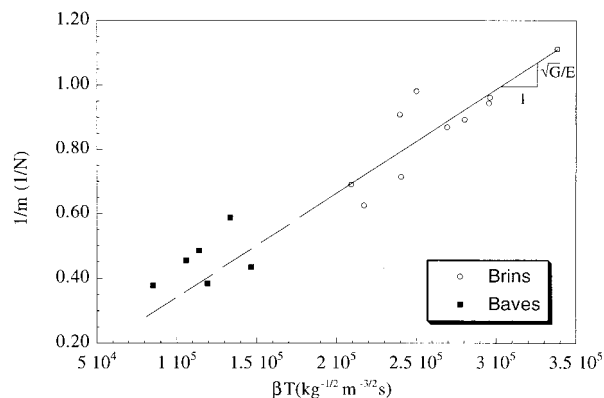


**Figure 8** Plots of  $(1/m)$  from tensile tests vs.  $\beta T$  from torsional tests. For brins,  $\beta = \alpha$ , and for baves  $\beta = \alpha/\sqrt{2}$ . Variables are defined in the context of eqs. (6) and (8) in the text. For both brins and baves, the slope of the plot is  $(\sqrt{G}/E)$ . A straight line has been fitted by least-squares regression to the brin data (solid line) and extrapolated through the bave data (broken line).

Although eq. (4) embodies an adequate description of the fiber cross-section, its accuracy in calculating  $G$  is, nevertheless, limited by the accuracy to which  $R$  can be measured. Small errors in the characterization of  $R$  are magnified when this quantity is raised to the fourth power.

It is useful, therefore, to consider the parameter  $E/\sqrt{G}$ , as this can, in principle, be measured without knowledge of the brin radius, if the approximation to a circular cross-section is valid. Because  $E$  depends on the measured radius as  $1/R^2$ , and  $G$  depends on measured radius as  $1/R^4$ ,  $E/\sqrt{G}$  can be expressed in terms of experimental parameters as:

$$\frac{E}{\sqrt{G}} = \frac{mT}{2\pi\sqrt{2\pi IL}} \quad (5)$$

which can be rewritten as

$$\frac{1}{m} = \frac{\sqrt{G}}{E} \frac{T}{2\pi\sqrt{2\pi IL}} \equiv \frac{\sqrt{G}}{E} \alpha T \quad (6)$$

where  $m$  is the slope of the force vs. strain curve in the linear elastic region of a tensile test, and reference to the parameter  $\alpha$  in the caption of Figure 8 facilitates the presentation of data. Figure 8 (open circles) shows values of  $(1/m)$  plotted as a function of  $[(T)/(1/2\pi\sqrt{2\pi IL})]$  for 10 samples of brin. A straight line, the slope of which is equal to  $(\sqrt{G}/E)$  according to eq. (6), was fitted to the

experimental results by the least-squares method. This leads to  $E/\sqrt{G} = 290,000 \pm 20,000$   $\sqrt{\text{Pa}}$ . Because it was not possible to perform both tensile and torsion tests on the same samples, tensile elastic modulus was inferred from a brin sample adjacent to each one used in the torsional pendulum. The average tensile modulus (Table I) is  $16 \pm 1$  GPa, so the inferred average shear modulus of brin is  $G = 3.0 \pm 0.8$  GPa.

A number of tests were also performed on baves, treating the material as two parallel non-interacting brins. Under this assumption, the use of eq. (4) on both brins in the bave leads to a modified version of eq. (5) for the parameter  $E/\sqrt{G}$ , which is now valid for baves:

$$\frac{E}{\sqrt{G}} = \frac{mT}{4\pi\sqrt{\pi IL}} \quad (7)$$

Equation (7) can be rewritten as:

$$\frac{1}{m} = \frac{\sqrt{G}}{E} \frac{T}{4\pi\sqrt{\pi IL}} \equiv \frac{\sqrt{G}}{E} \frac{\alpha}{\sqrt{2}} T \quad (8)$$

In this case, a plot of  $(1/m)$  vs.  $[(T)(1/4\pi\sqrt{\pi IL})]$  is required to yield a straight line of slope  $(\sqrt{G}/E)$ . The plotted data (filled squares in Fig. 8) lie close to the extrapolation of the line fitted to the data for single brins, confirming that brins and baves exhibit equivalent mechanical behavior when they are compared on the basis of parameters that are independent of the cross-sectional area. The comparison effected in Figure 8 is insensitive to the presence of sericin, which only changes the fiber radius without contributing significantly to the intrinsic mechanical properties of the fiber.

Literature data for the shear modulus of silkworm silk are sparse.<sup>14,17,18</sup> Among these, the careful work of Meredith<sup>14</sup> stands out; the shear modulus of a number of natural fibers was obtained with a torsional pendulum, and the effect of fiber shape was taken into account. A value of  $G = 2.4$  GPa was obtained for silkworm bave. The difference between that result and ours (3.0 GPa) is unsurprising, given that Meredith estimated an average fiber radius from measurements of mass and density, without the ability to compensate for residual sericin. Forty-five years after Meredith's work, we have benefitted from ready access to scanning electron microscopy, which makes characterization of local sample geometry possible.

Finally, we note that our values for the tensile and shear modulus of silkworm brin lead to  $E/G = 5.3 \pm 0.3$ . This parameter is often used as a measure of microstructural anisotropy, because  $E$  is increased while  $G$  is decreased by molecular alignment.<sup>19</sup> The maximum value of  $E/G$  for isotropic material (requiring a Poisson's ratio of 0.5) is 3. Our value of 5.3 for *B. mori* brin is higher than the literature value<sup>19</sup> of 3.9, again reflecting the fact that we have minimized the contribution of amorphous sericin to our results. Interestingly, the value of  $E/G$  for nylon, a polymer initially developed to mimic the properties of silk,<sup>20</sup> is approximately 5.8.<sup>19</sup>

## CONCLUSIONS

The tensile modulus ( $16 \pm 1$  GPa) and conventional yield stress ( $230 \pm 10$  MPa) of *B. mori* silk, obtained from tests performed on single brins, are significantly higher than the literature values that are reported for bave. The principal source of this difference is the presence of sericin in bave; the sericin contributes to sample cross-section, but adds little to the fiber's ability to resist tensile deformation. By using a scanning electron microscope to characterize the cross-section of brins tested, we were able to minimize the contribution of sericin to our results, and to take into account the sample-to-sample variability in cross-sectional geometry. The two brins in a bave contribute equally and independently to the tensile load-bearing ability of the material.

Measurements performed with a torsional pendulum can be combined with tensile load-extension data to obtain a value of  $E/\sqrt{G}$  that is not sensitive to sample cross-sectional dimensions or, therefore, to the presence of sericin. The value of  $E$  measured for brin can be used together with this procedure to obtain  $G = 3.0 \pm 0.8$  GPa and  $E/G = 5.3 \pm 0.3$  for brin. The latter value indicates a mechanical and, therefore, microstructural anisotropy comparable to that of nylon.

## REFERENCES

1. Iizuka, E. *J Appl Polym Sci* 1985, 41, 173.
2. Magoshi, J.; Nakamura, S. *J Appl Polym Sci* 1985, 41, 187.
3. Ito, H.; Muraoka, Y.; Yamazaki, T. Imamura, T.; Mori, H.; Ichida, M.; Sumida, M.; Matsubara, F. *Textile Res J* 1995, 65, 755.

4. Nadiger, G. S.; Halliyal, V. G. *Colourage* 1984, 31(20), 23.
5. Nakamae, K.; Nishino, T.; Ohkubo, H. *Polymer* 1989, 30, 1243.
6. Kawahara, Y.; Shioya, M.; Takaku, A. *J Appl Polym Sci* 1996, 61, 1359.
7. Kaplan, D.L.; Lombardi, S. J.; Muller, W. S.; Fossey, S. A. In *Biomaterials. Novel Materials from Biological Sources*; Byrom, D., Ed. Stockton Press: New York, 1991, p. 1.
8. Lucas, F.; Shaw, J. T. B.; Smith, S. G. *J Textile Inst* 1955, 46, T440.
9. Pérez-Rigueiro, J.; Viney, C.; Llorca, J.; Elices, M. *J Appl Polym Sci* 1998, 70, 2439.
10. Kaplan, D.; Adams, W. W.; Farmer, B.; Viney, C. In *Silk Polymers*; Kaplan, D.; Adams, W. W.; Farmer, B.; Viney, C., Eds. American Chemical Society: Washington, DC, 1994, p. 2.
11. Dunaway, D. L.; Thiel, B. L.; Srinivasan, S. G.; Viney, C. *J Mater Sci* 1995, 30, 4161.
12. Ward, I. M.; Hadley, D. W. *An Introduction to the Mechanical Properties of Solid Polymers*; John Wiley & Sons: Chichester, 1993.
13. Work, R. W. *Textile Res J* 1977, 47, 650.
14. Meredith, R. *Textile Res J* 1954, 7, 1489.
15. Fouda, I. M.; El-Tonsy, M.M. *J Mater Sci* 1990, 25, 4752.
16. Shen, Y.; Johnson, M. A.; Martin, D. C. *Macromolecules* 1998, 31, 8857.
17. Wagner, E. *Mechanisch-technologische Textilprüfungen*, 6 Auflage, Fr. Staats GmbH / Dr. Spohr-Verlag, Wuppertal-Barmen, 1953.
18. Zemlin, J. C. *A Study of the Mechanical Behavior of Spider Silks*; Report no. 69-29-CM (AD 684333), U.S. Army Natick Laboratories: Natick MA, 1968.
19. Warner, S. B. *Fiber Science*; Prentice-Hall: Englewood Cliffs, NJ, 1995.
20. Morawetz, H. *Polymers: The Origins and Growth of a Science*; John Wiley & Sons: New York, 1985.